Drug Design, Development and Therapy

Dovepress
open access to scientific and medical research

Open Access Full Text Article

ORIGINAL RESEARCH

"PFH/AGM-CBA/HSV-TK/LIPOSOME-Affibody": Novel Targeted Nano Ultrasound Contrast Agents for Ultrasound Imaging and Inhibited the Growth of ErbB2-Overexpressing Gastric Cancer Cells

Houren Zhou[1], Hui Liu[2], Yue Zhang[3], Ying Xin[3], Chi Huang[3], Mingzhong Li[4], Xiaoyun Zhao[2], Pingtian Ding[2], Zhijun Liu[3]

[1]Ultrasound Department, The Second Affiliated Hospital of Dalian Medical University, Dalian, People's Republic of China; [2]School of Pharmacy, Shenyang Pharmaceutical University, Shenyang, People's Republic of China; [3]Ultrasound Department, Shengjing Hospital, China Medical University, Shenyang, People's Republic of China; [4]School of Pharmacy, De Montfort University, Leicester, LE1 9BH, UK

Correspondence: Zhijun Liu, Ultrasound Department, Shengjing Hospital, China Medical University, 36 Sanhao Street, Shenyang, Liaoning Province, 110004, People's Republic of China, Email liuzj1@sj-hospital.org

Objective: Gastric cancer is one of the most lethal malignancies in the world. However, the current research on the diagnosis and treatment of nano-ultrasound contrast agents in the field of tumor is mostly focused on breast cancer, ovarian cancer, prostate cancer, liver cancer, etc. Due to the interference of gas in the stomach, there is no report on the treatment of gastric cancer. Herpes simplex virus thymidine kinase/ganciclovir (HSV-TK/GCV) therapy system is the most mature tumor suicide gene in cancer treatment. At the same time, in order to improve its safety and efficiency, we designed a gastric tumor targeted ultrasound-triggered phase-transition nano ultrasound contrast agent PFH/AGM-CBA/HSV-TK/Liposome (PAHL)-Affibody complex.

Methods: In our study, guanidinylated SS-PAAs polymer poly(agmatine/N, N′-cystamine-bis-acrylamide) (AGM-CBA) was used as a nuclear localization vector of suicide gene to form a polyplex, perfluorohexane (PFH) was used as ultrasound contrast agent, liposomes were used to encapsulate perfluorohexane droplets and the polyplexes of AGM-CBA/HSV-TK, and affibody molecules were conjugated to the prepared PAHL in order to obtain a specific targeting affinity to human epidermal growth factor receptor type 2 (ErbB2) at gastric cancer cells. With the aid of ultrasound targeted microbubble destruction technology and the nuclear localization effect of AGM-CBA vector, the transfection efficiency of the suicide gene in gastric cancer cells was significantly increased, leading to significant apoptosis of gastric cancer cells.

Results: It was shown that PAHL-Affibody complex was nearly spherical with an average diameter of 560 ± 28.9 nm, having higher and specific affinity to ErbB2 (+) gastric cells. In vitro experiments further confirmed that PAHL could target gastric cancer cells expressing ErbB2. In a contrast-enhanced ultrasound scanning study, the prepared ultrasound-triggered phase-change nano-ultrasound contrast agent, PAHL, showed improved ultrasound enhancement effects. With the application of the low-frequency ultrasound, the gene transfection efficiency of PAHL was significantly improved, **thereby** inducing **significant** apoptosis in gastric cancer cells.

Conclusion: This study constructs PFH/AGM-CBA/HSV-TK/Liposome-Affibody nano ultrasound contrast agent, which provides new ideas for the treatment strategy of ErbB2-positive gastric cancer and provides some preliminary experimental basis for its inhibitory effect.

Keywords: Herpes simplex virus thymidine kinase/ganciclovir, poly (agmatine/N, N′-cystamine-bis-acrylamide), ErbB2 targeting, gene transfection, low-frequency ultrasound

Introduction

Gastric cancer is one of the most lethal malignancies in the world.[1] Due to lack of specific early warning symptoms or effective examination methods, gastric cancer is often at a later stage when it is diagnosed. For patients with unresectable late or metastatic gastric cancer and recurrence after surgery, the reported median survival time of traditional chemotherapy in a gastric cancer was

Received: 14 December 2021
Accepted: 4 May 2022
Published: 18 May 2022

only about 11 months.[2] Therefore, new treatment protocols must be developed. With the advance of molecular biology, more and more gene therapies are being used for cancer treatments. Among them, suicide gene therapy is considered as a potential weapon against tumors due to its high selectivity for tumor cells.[3] Herpes simplex virus thymidine kinase/ganciclovir (HSV-TK/GCV) treatment system is a good exemplar of such a suicide gene therapy, currently the most commonly used, mature and effective suicide gene therapy.[3–6]

Although suicide gene therapy has unique theoretical advantages, in order to achieve the desired clinical outcome in a gene therapy, effect in actual treatment, anti-tumor suicide genes need to be transferred to the tumor site efficiently and safely by a carrier, which can be either a virus vector or a non-virus vector.[3] Common gene delivery systems include virus vectors and non-virus vectors. Despite higher transfection efficiencies, virus vectors can cause many problems, such as immune response, production of wild-type viruses, and possible tumorigenicity.[7] A non-virus delivery vector would be a potential solution to avoid the problem of immunogenicity, although it suffers from low transfection efficiencies.[8] In our previous studies, a nuclear localization vector AGM-CBA was designed to deliver HSV-TK suicide gene into cancer cells, which was synthesized from polymerization of Agmatine (AGM) and N, N′-cystamine-bis- acrylamide (CBA). It has been demonstrated that AGM-CBA is of lower cytotoxicity, higher transfection efficiency, and excellent nuclear localization effect as a gene delivery carrier in various applications.[9–11]

In recent years, nano ultrasound contrast agents (UCAs) in combination with ultrasound-targeted microbubble destruction (UTMD) technology have been developed to improve the transfection efficiency of genes in gene therapies.[12–14] Nano UCAs as gene carriers can overcome the problem of traditional microbubbles (size of 1–5 μm), which are usually limited to the vascular pool. Due to the smaller particle size, typically in the range of 380−780 nm, Nano UCAs can enter the tumor tissue directly through the gap between tumor neovascular endothelial cells.[15] At physiological temperature (37 °C), these nano-droplets are kept in the liquid state. However, under high sound pressure, water droplet acoustic vaporization (ADV) can take place to change nano-droplets into microbubbles.[16] These microbubbles can be easily observed for ultrasound imaging due to increased acoustic impedance. Once reaching the target tissues, the gene-bearing microbubble contrast agent could be further broken by low-frequency ultrasound to form small holes in the cell membranes, promoting the exogenous genes to enter the tumor tissues by cavitation effects and acoustic pores.[17] It was reported that gas-phase perfluorocarbons encapsulated in microbubbles were easily leaked from the shell materials of the microbubbles under physical denaturation and ultrasonic treatment, resulting in short blood circulation life.[18]

It has been reported that 13%−16% of patients with gastric cancer show an ErbB2 gene amplification and protein overexpression.[19] A specific antibody is usually attached to ErbB2shells to form ErbB2-targeted nano UCAs, which can specifically correspond to the ErbB2 receptor expressed by the tumor, resulting in accumulation of HS-TK at the tumor targeting sites.[20–23]

In this study, the guanidinylated SS-PAAs polymer, AGM-CBA was used as the nuclear localization vector of the HSV-TK suicide gene and the ErbB2 targeted nano UCAs was used as the gene targeting vector. Both nuclear localization effect of AGM-CBA and UTMD technology vector were used to jointly improve the transfection efficiency of the HSV-TK genes in the gastric cancer cells, leading to the significant apoptosis of gastric cancer cells. Liposomes were used to encapsulate perfluorohexane droplets and the polyplexes of AGM-CBA/HSV-TK to maintain the stability (Schematic diagram of principle is shown in Scheme 1).

Materials and Methods

Materials

Poly(agmatine/N, N′-cystamine-bis-acrylamide) (AGM-CBA) was synthesized according to our previous report.[11] Herpes simplex virus thymosin kinase (HSV-TK) was purchased from the Gamma gene (Suzhou, China). 1,2-dipalmitoyl-snglycero-3-phosphocholine (DPPC), 1,2-distearoyl-sn-glycero-3- phosphoethanolamine-N- [biotinylated (polyethylene glycol) −2000] (biotinylated DSPE-PEG (2000)) were purchased in powder form from Avanti Polar Lipids Inc. (Alabaster, AL). Dimethyl sulfoxide (DMSO), MTT (3-(4,5-dimethylthiazol-2-yl)-2,5-diphenyl tetrazolium bromide), cholesterol and ganciclovir were purchased from Sigma-Aldrich (St. Louis, MO, USA). Perfluorohexane (PFH) was purchased from Shanghai Fluoro Technology (Shanghai, China). Streptavidin was purchased from Beijing Boaosen

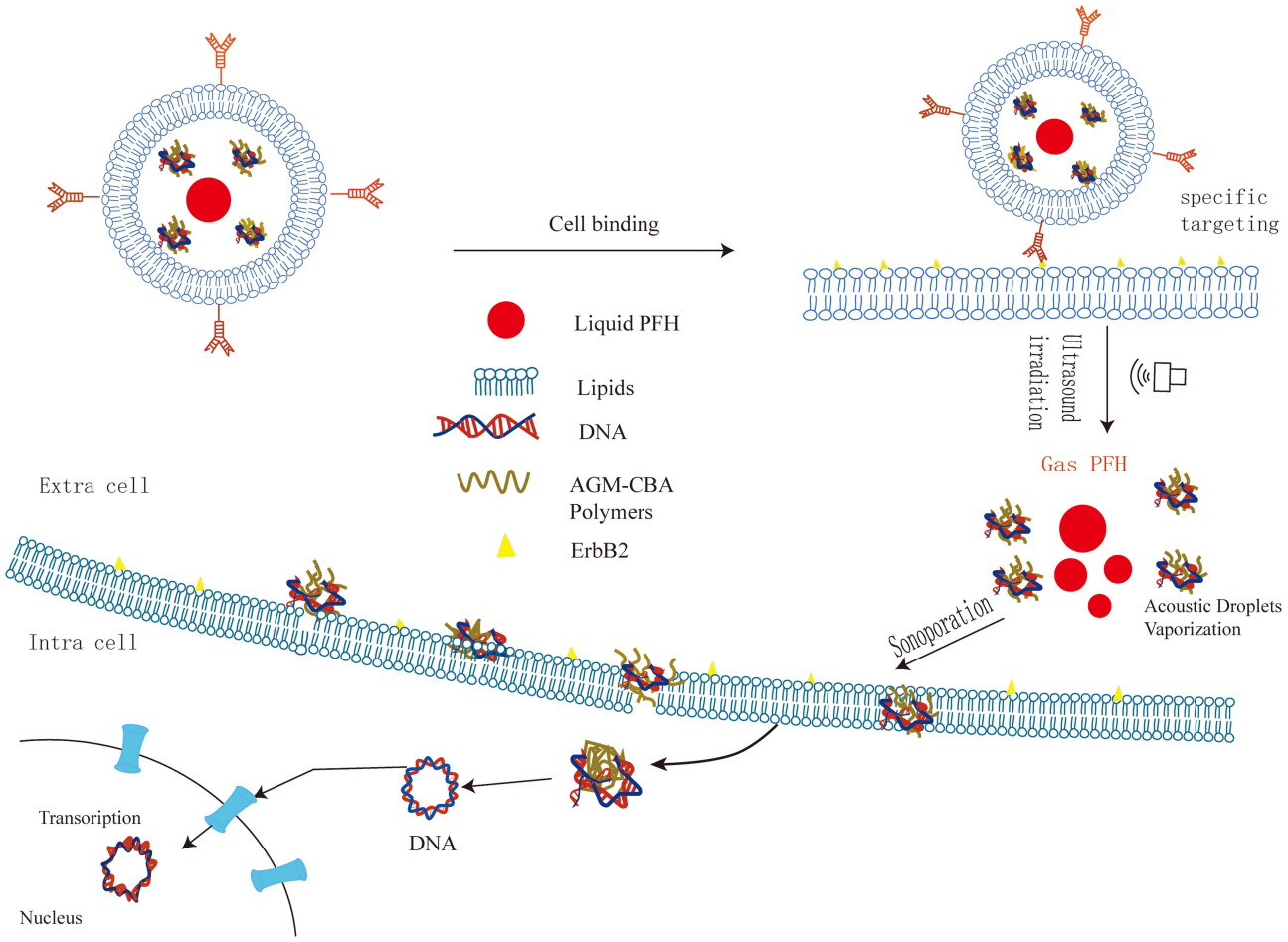

Scheme 1 Schematic Diagram of the PAHL for the Targeting Ultrasound-Assisted Gene Transfection.

Biotechnology Co., Ltd. (Beijing, China). Biotinylated anti-ErbB2 Affibody was purchased from Abcam (California, USA). Phosphate-buffered saline (PBS, pH: 7.4) and trypsin were purchased from Beijing Solibao Technology Co., Ltd. (Beijing, China). Ethidium bromide (EB) was purchased from Tiangen Biotech Co., Ltd. (Beijing, China). DiI fluorescent dye was purchased from Hangzhou Biyuntian Biotechnology Research Institute (Hangzhou, China). Hochest 33,342 were obtained from Beyotime Institute of Biotechnology (Haimen, China). Label IT Tracker Reagent Intracellular Nucleic Acid Localization Kits (MIR 702, Mirus) were obtained from Beijing Xinbosheng Biotechnology Co., Ltd. (Beijing, China). Both NCI-N87 and MGC-803 gastric cancer cells were purchased from the Cell Bank of the Chinese Academy of Sciences (Shanghai, China). Fetal bovine serum (FBS) was purchased from Thermo Fisher Oxoid (Basingstoke, UK). DMEM and RPMI 1640 medium were purchased from Corning (New York, NY, USA).

Preparation and Evaluation of the Polyplexes (AGM-CBA/HSV-TK)

The cationic non-viral gene delivery vector (AGM-CBA) was selected as the vector of HSV-TK. The weight ratio of AGM-CBA to HSV-TK was chosen as 9:1 in this study based on our previous work.[10] A 90 μg AGM-CBA solution at a concentration of 20 mg/mL and a solution containing 10 μg of HSV-TK at a concentration of 300 μg/mL was prepared, respectively. Subsequently, an equal volume of AGM-CBA solution with different concentrations was carefully added to an equal volume of HSV-TK solution. Then, the solution mixture was gently mixed, and left at room temperature for 30 minutes to form polyplexes of AGM-CBA/HSV-TK. The particle size and zeta potential of the polyplexes of AGM-CBA /HSV-TK (containing 10 μg HSV-TK) were measured by Malvern Zetasizer Nano ZS unit (Zetasizer Nano ZS90, Marvin Company). The polyplex samples were measured three times in parallel. The prepared positively charged polyplexes of AGM-CBA/HSV-TK (containing 10 μg HSV-TK) was stored at 4 °C for future use.

Construction of PFH/AGM-CBA/HSV-TK/Liposome (PAHL) Nano Ultrasound Contrast Agent (UCA)

PAHL nano UCA was prepared by a thin film hydration method in conjunction with acoustic vibration.[24] DPPC (8.8 mg), cholesterol (3.0 mg), and negatively charged Biotin-DSPE-PEG2000 (2.8 mg) were mixed in a molar ratio of 60:40:5, then dissolved with 2 mL anhydrous ethanol. Then, in a rotary evaporator, rotary evaporation of the lipid mixture was performed at 37 °C and 120 rpm for 15 minutes, and nitrogen was blown dry for 30 minutes to obtain a dried lipid film. The dried film mixture was hydrated with 2 mL of a hydration solution consisting of the polyplexes of AGM-CBA/HSV-TK and PBS, and a liposome suspension containing the polyplexes of AGM-CBA/HSV-TK was prepared. The suspension was placed in a 10 mL polyethylene tube, and 80 μL of PFH was added in a dropwise manner. Under a full ice bath condition, the mixture of liposomal suspension and PFH was oscillated for 6 min using a mechanical oscillator (PS3100, Xi'an, China). The mixture was then placed in a high-speed centrifuge, and centrifuged three times (8000 rpm for 2 min each time). After centrifugation, the supernatant was removed, and then 2 mL of PBS was added and mixed with the precipitate by a vortex mixer, resulting in a micro-ultrasound contrast agent. This newly formed micro-ultrasound contrast agent was extruded through an extruder (Lipo Fast, AVESTIN, Canada) with a polycarbonate film of 1 μm and then 400 nm for 21 times, to obtain the PAHL nano UCA. Size distribution and zeta potential of the PAHL nano UCA were measured using a Malvern Zetasizer Nano ZS unit. The PAHL nano UCA samples were measured three times in parallel. In this study, PAHL nano UCA without PFH was also prepared in a similar manner as a control.

Construction of PFH/AGM-CBA/HSV-TK/Liposome (PAHL) Affibody as Nano Ultrasound Contrast Agent (UCA)

To couple the PAHL nano UCAs carrying HSV-TK with anti-ErbB2 Affibody molecules, an avidin-biotin method was used. The parent suspension of 100 μL PAHL nano UCA was diluted in 900 μL PBS, then 30 μL of streptavidin (5 mg/mL) was added and placed at 4 °C for 30 min. After that, 700 μL of PBS was added. The mixture was centrifuged at 8000 rpm for 2 min. The supernatant was discarded, and the precipitate of the bottom layer was retained. The precipitate was then washed three times to clean out the excess streptavidin. Next, 2 μL (25 μg/mL) of biotinylated anti-ErbB2 Affibody (25 μg/mL) was added to the cleaned PHAL nano UCA suspension, and was placed at 4 °C for 30 min with slight shaking. The conjugated PAHL-Affibody nano-UCA was then washed three times with PBS. In addition, PAHL nano UCA without anti-ErbB2 Affibody was prepared in the study as a control. Both PAHL nano UCA with and without Affibody were finally sterilized by CO60 irradiation for 30 min and then stored at 4 ° C for future use.

Characterization of PAHL-Affibody Nano UCA

The prepared PAHL-Affibody nano UCA was observed with an ultra-high resolution field emission scanning electron microscope (SEM, Hitachi Regulus 8100, Japan). The structures of PAHL-Affibody nano UCA with and without PFH were analyzed by transmission electron microscope (TEM, JEM-1200EX, Japan). Size distribution and zeta potential of the PAHL-Affibody nano UCA were measured using a Malvern Zetasizer Nano ZS unit. The PAHL-Affibody nano UCA samples were measured three times in parallel.

The encapsulation efficiency of PAHL was determined as previously reported.[11] The supernatant collected by high-speed centrifugation in section 2.3 was collected in a polyethylene tube, which was the unencapsulated polyplexes of AGM-CBA/HSV-TK. Then, an equal volume of heparin sodium (1000U/L) was added and incubated at 37 °C for 30 min, HSV-TK was replaced by heparin from the polymer carrier AGM-CBA. The fluorescence intensity of the resulting mixture was measured by a microplate reader (SpectraMax M3; Molecular Devices LLC, Sunnyvale, CA, USA). The excitation wavelength was set to 510 nm, and the emission wavelength was 595 nm. The weight of unencapsulated HSV-TK was calculated from the standard curve of HSV-TK solution. The encapsulation efficiency (EE) of PAHL to HSV-TK was calculated according to the following formula:[11,25]

$$EE\ (\%)=(Mi - Mu)/Mu \times 100\ \%$$

Mi and Mu were the weights of the HSV-TK initially added and the unencapsulated HSV-TK, respectively.

In addition, flow cytometry was carried out to determine the encapsulation efficiency of the polyplexes of AGM-CBA /HSV-TK by the nano UCAs with a flow cytometer (BD, Biosciences, Sunnyvale, CA, USA).

Specific Targeting of ErbB2 (+) Gastric Cancer Cells by PAHL-Affibody Nano UCA in vitro

In the process of preparing PAHL nano UCA, 3.0 μL DiI fluorescent dye (5 mmol/L) was added to the process of dissolving phospholipid in order to track PAHL. The rotating steam flask was wrapped in aluminum foil with gentle shaking to make PAHL-fluorescent dye stable and evenly mixed. The other preparation steps were the same as described in sections 2.3 and 2.4.

Human gastric cancer cells (NCI-N87) of ErbB2 (+) was inoculated into RPMI1640 medium containing 10% FBS, and human gastric cancer cells (MGC-803) of ErbB2 (-) was inoculated into DMEM containing 10% FBS. The cells were cultured in an incubator at 37 °C, suitable humidity and 5% CO2. The NCI-N87 cells and MGC-803 cells were grown to 70–80% of confluency. As for NCI-N87 cells, the culture medium was discarded and the cells were gently washed 3 times with sterile PBS, and then 300 μL (7.3 mg/mL) of sterile PAHL-Affibody nano UCAs was added. As a control, 300 μL (7.3 mg/mL) of sterile PAHL nano UCA without Affibody was also tested. In addition, ErbB2 (-) MGC-803 cells were used in the study as another control. The MGC-803 cells were gently washed three times with sterile PBS, 300 μL (7.3 mg/mL) of sterile PAHL-Affibody nano UCA was used to treat the MGC-803 cells. After all the treatments, the culture dishes were shaken slightly and incubated at room temperature for 30 min. The culture dishes were then washed several times gently with sterile PBS. Each culture dish was observed and photographed with a laser confocal microscope (Carl Zeiss LSM710, Oberkochen, Germany).

Flow cytometry was used to observe the binding rate of PAHL-Affibody nano UCA to NCI-N87 cells in this study. NCI-N87 cells were cultured and trypsinized, as described in section 2.6, and then collected in sterile test tubes, with each tube containing 2×10^5 cells. Test tube 1 was a blank control. Test tube 2 was added with 300 μL (7.3 mg/mL) of sterilized PAHL nano UCA without Affibody. Test tube 3 was filled with 300 μL (7.3 mg/mL) of sterilized PAHL-Affibody nano UCAs. Each test tube was centrifuged at low-temperature and a speed of 20 × g for 3 min. The supernatant was discarded, and the cells were resuspended in 1 mL of PBS. The cells were gently blown to form a homogeneous dispersion suspension, and then analyzed by flow cytometry. The above experiment was repeated at least three times.

Stability Test of PAHL-Affibody Nano UCA

The prepared PAHL-Affibody nano UCAs (100 μL) was added into polyethylene tube containing 1 mL of PBS and stored at 4 ° C for stability test. Particle size and zeta potential of the nano UCAs were measured by Malvern Zetasizer Nano ZS unit at 0 d, 7 d, 14 d and 30 d, respectively. The above experiment was repeated at least three times.

In vitro Ultrasound Imaging of PAHL-Affibody Nano UCA

Contrast-enhanced ultrasound (CEUS) imaging was performed using a Philips iu22 ultrasound system (Royal Phillips of Holland). The probe was a linear array probe L9-3, and the frequency was set as 10 MHz.

Degassed water (2 mL) and PAHL-Affibody UCA (2 mL) samples were, respectively, placed in a Pasteur plastic pipette. The two samples were heated to 37 ° C or 65 ° C for 20 seconds, and then immediately placed in a pure water tank to acquire ultrasound images in contrast mode. In addition, the PAHL-Affibody UCA was placed under ultrasound irradiation under the previously determined mechanical index conditions, and the CEUS images were recorded from 0 to 20 min to examine its relative stability during ultrasound imaging.

Optimization of Time Parameters of Low Frequency Ultrasound for Irradiation of NCI-N87 Gastric Cancer Cells

NCI-N87 gastric cancer cells were routinely cultured. The cells grown in the logarithmic phase were taken to form a density of 5×10^4/m1 cell suspension and placed into a sterile polyethylene tube (2 mL/tube). The power of the low-

frequency ultrasound instrument was fixed at 2 W, and the frequency was set as 650 KHz. The radiation time parameters were set as 0, 30, 40, 50, 60, 70, 80 and 90 s, respectively. After NCI-87 cells were treated by the ultrasound irradiation, the cells were seeded in 96 plates at 200 μL/well, with 5 replicates in each group, and cultured overnight. After 24 hours, 20 μL MTT (5 mg/mL) was added to each well without light, and then the cells were placed at 37°C for 4 h to form a formazan crystal. The culture medium containing the MTT was discarded. Subsequently, 200 μL of DMSO was added to each well, and the formazan crystal was dissolved by being oscillated for 3 minutes. The absorbance value of each well was measured at the 490 nm wavelength by a microplate reader (Infinite F200 PRO, TECAN, Switzerland). The cell viability was calculated as previously described.[26]

Nuclear Localization Effect of PAHL-Affibody Nano UCA

According to the manufacturer's instructions of the Label® IT™ Tracker Intracellular Nucleic Acid Localization Kit, HSV-TK was labeled with Cy5. Using the Cy5 labelled HSV-TK, we prepared the polyplexes of AGM-CBA/HSV-TK, PAHL nano UCA with Affibody, and PAHL nano UCA without Affibody according to sections 2.2, 2.3 and 2.4.

NCI-N87 cells were seeded at a density of 2×10^5 cells/dish on the cover slides in petri dishes and grown overnight. The medium was changed to a fresh serum-free medium before transfection study. Subsequently, 100 μL of polyplexes of AGM-CBA/HSV-TK, PAHL nano UCA with Affibody, or PAHL nano UCA without Affibody was added to each well, and then subjected to the low-frequency ultrasound irradiation. The low-frequency ultrasound irradiation condition was set as 650 kHz, 1.5 W/cm2, and 60 s of irradiation time, which was optimized in our study. The NCI-N87 cells were then cultured at 37 °C for 4 h. The cells were washed with PBS for three times, and then incubated with 8 μg/mL of Hoechst 33,342 to stain the cell nuclei, and then fixed with 4% paraformaldehyde (1.5 mL/dish) for 30 min. Lastly, the coverslips with cells were placed on the glass slides for further analysis. Zeiss Axiovert 200 M inverted microscope coupled with Zeiss LSM 510 scanning confocal head (Carl Zeiss Co., Ltd., Jena, Germany) was used to analyze the nuclear localization effect of PAHL-Affibody nano UCA.

Inhibitory Effect of PAHL-Affibody Nano UCA Combined with Low-Frequency Ultrasound on the Proliferation of ErbB2 (+) Gastric Cancer Cells

First, the toxic effects of different concentrations of ganciclovir (GCV) on ErbB2 (+) gastric cancer cells (NCI-N87) were investigated to determine the optimal ganciclovir concentration. After NCI-87 cell growth was stable, the cells were seeded in a 96-well plate with a density of 5000 cells per well. Six concentrations of GCV were tested, including 0 (as a control), 20, 50, 100, 200, 500, 1000, 2000, 5000 μg/mL. After the cells were cultured for 48 h, 20 μL MTT (5 mg/mL) was added into each well. After 4 h, the culture medium with MTT was discarded, and then 200 μL DMSO was added. The absorbance value of each well was measured at a wavelength of 490 nm by a microplate reader. The effects of different concentrations of GCV on cell survival were evaluated, and the optimal concentration of GCV was determined afterwards.

Subsequently, we evaluated the inhibitory effect PAHL-Affibody nano UCA on the proliferation of ErbB2 (+) gastric cancer cells. NCI-N87 cells were seeded at a density of 5×10^4 cells per well, and then cultured overnight. NCI-N87 cells were then transfected with the following four treatments, including Treatment A – blank nano UCA (without AGM-CBA /HSV-TK and ultrasound irradiation), Treatment B – Affibody-connected ErbB2 targeted blank nano UCA (without AGM-CBA/HSV-TK and ultrasound irradiation), Treatment C - PAHL-Affibody nano UCA (without ultrasound irradiation), Treatment D - PAHL-Affibody nano UCA (with ultrasound irradiation). In this study, the low-frequency ultrasound irradiation condition was set as 650 kHz, 1.5 W/cm2, and 60 s of irradiation time, which was optimized in our study. After 4 hours of transfection experiment, the NCI-87 cells were changed to a fresh, complete medium, and kept on growing for 24 hours. And then, the optimal concentration of GCV was added to the cells. After 48 h of incubation, MTT toxicity study was carried out to evaluate the cell survival rate as described in section 2.9. In addition, the apoptosis of gastric cancer cells was evaluated by a flow cytometer (BD, Biosciences, Sunnyvale, CA, USA).

Statistical Analysis

Statistical analysis was performed using independent sample *t*-test (comparison of two groups) and multivariate analysis of variance (ANOVA). When the p value was <0.05, the difference was statistically significant.

Results

Characterization of PAHL-Affibody Nano UCA

The particle size and zeta potential of the polyplexes of AGM-CBA/HSV-TK and the PAHL nano UCA were determined by Malvern Zetasizer Nano ZS unit. The particle size and the zeta potential of the former were found to be 102.3 ± 2.3 nm and 24.7 ± 0.9 mV, and the particle size and the zeta potential of the latter were found to be 422.4 ± 4.3 nm and −6.2 ± 0.3 mV. The surface morphology of PAHL-Affibody nano UCA was evaluated by SEM, indicating a uniform and smooth spherical structure (Figure 1A). Figure 1B and C showed typical TEM images of AGM-CBA/HSV-TK/Liposome-Affibody and PAHL-Affibody nano UCA. The dark matter (red solid circle) in the center of the sphere in Figure 1C shows the presence of liquid PFH. The center of PAHL in the absence of liquid PFH appeared white. Furthermore, the particle size, size distribution, and zeta potential of PAHL-Affibody nano UCA were determined by Malvern Zetasizer Nano ZS unit. The results showed that the average particle size was 560 ± 4.8 nm and the size distribution was narrow (PDI = 0.197 ± 0.038) (Figure 1D). The surface zeta potential was found to be -11.2 ± 0.5 mV (Figure 1E). The encapsulation efficiency of HSV-TK in liposomes was excellent (about 68.7%), which was determined by fluorescence spectrophotometry. In addition, the binding rate of the double layered phospholipid and the polyplexes of AGM-CBA/HSV-TK was determined to be 89.2% determined by flow cytometry (Figure 2), which indirectly proved its high encapsulation efficiency for the polyplexes.

Specific Targeting of ErbB2 (+) Gastric Cancer Cells by PAHL-Affibody Nano UCA in vitro

Affibody is a new type of synthetic affinity ligand that is similar to antibody in function. However, there is no corresponding fluorescent secondary antibody for Affibody, and there is no easy approach to directly detect the connection between Affibody and nano UCAs. Therefore, by detecting the connection between the PAHL with red fluorescent dye imbedded in the liposomal components and ErbB2 (+) gastric cancer cells, we indirectly tested the connection between Affibody and PAHL, and verified its targeting ability to ErbB2 (+) gastric cancer cells. In this study,

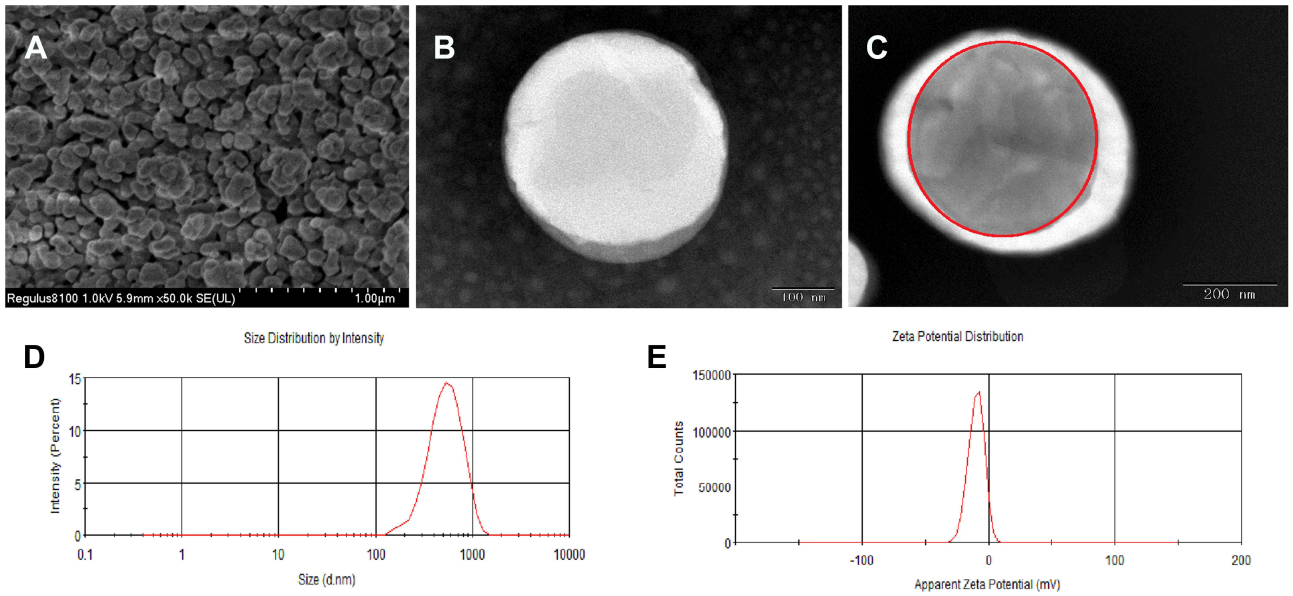

Figure 1 Characterization of PAHL-Affibody nano UCA. (**A**) SEM image of PAHL-Affibody nano UCA (scale bar, 1 μm). (**B**) TEM images of AGM-CBA/HSV-TK/Liposome-Affibody (scale bar, 200 nm). (**C**) TEM images of PAHL-Affibody nano UCA (scale bar, 200 nm). The dark mass in the center of the spheres was the PFH inner core (indicated by red solid circle). (**D** and **E**) Size distribution and Zeta potential of PAHL-Affibody nano UCA.

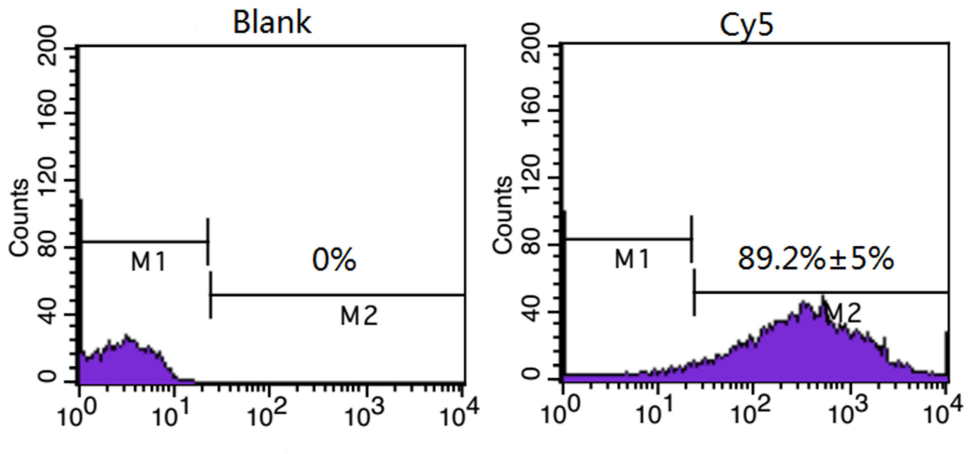

Figure 2 FCM analysis of PFH/Liposome-Affibody (without the polyplexes of AGM-CBA/HSV-TK) (left) and PAHL-Affibody (HSV-TK stained by Cy5 (right).

we selected ErbB2 (+) gastric cancer cells (NCI-N87) and ErbB2 (-) gastric cancer cells (MGC-803). It was observed under laser scanning confocal microscope that a large amount of PAHL with red fluorescence was connected to the NCI-N87 cells. However, only a small amount of PAHL with red fluorescence was accumulated in the MGC-803 cells. When NCI-N87 cells was treated by PAHL nano UCAs without coupling to Affibody, there was also little accumulation of PAHL nano UCAs with red fluorescence in the cells (Figure 3A).

The targeted binding rate of PAHL and gastric cancer cells was analyzed by flow cytometry. The results showed that the targeted binding rate of PAHL-Affibody nano UCA to ErbB2 (+) gastric cancer cells (NCI-N87) was 56.6%, while that of PAHL nano UCAs without Affibody connection with NCI-N87 cells was only 0.6% (Figure 3B). There was a significant statistical difference between the two values ($p < 0.05$), thus further confirming the high targeting ability of the PAHL-Affibody nano UCA to the ErbB2 (+) gastric cancer cells.

In vitro Storage Stability of PAHL-Affibody Nano UCA

PAHL-Affibody was stored at 4°C, and its particle size and zeta potential were measured at 0, 7, 15, and 30 days. The particle size and zeta potential of PAHL are shown in Figure 4A and B. It showed that there were no significant changes in its particle size and zeta potential ($p > 0.05$), indicating that the prepared negatively charged PAHL-Affibody nano UCA was at least stable at 4 °C for 30 days.

In vitro Ultrasound Imaging of PAHL-Affibody Nano UCA

First of all, we took degassed water as a control to investigate the effect of temperature on the contrast effect. It was found that the ultrasound contrast effect of PAHL –Affibody nano UCA at 65°C was significantly better than that at room temperature (25°C), while the ultrasound contrast effect of the control (degassed water) had no obvious difference between these two temperatures (Figure 5A).

We also evaluated the response of PAHL to different mechanical indexes (MI), and the range of ultrasonic mechanical indexes examined was 0.03 to 1.31. It can be observed that with the mechanical index ranging from 0.04 to 0.37, the ultrasonic image was gradually lightened. However, when the mechanical index continued to increase to 1.31, the ultrasound image gradually became darkened (Figure 5B). It was determined that PAHL-Affibody nano UCA could maintain a stability for more than 20 minutes under ultrasound irradiation with a mechanical index of 0.09 (Figure 5C).

Determination of the Optimal Irradiation Time of Low Frequency Ultrasound Instrument

The effects of irradiation time of low-frequency ultrasound on the cell survival were evaluated by an MTT test. The irradiation times tested were set as 30, 40, 50, 60, 70, 80 and 90 s. The ultrasound intensity was predetermined as 1.5 w/

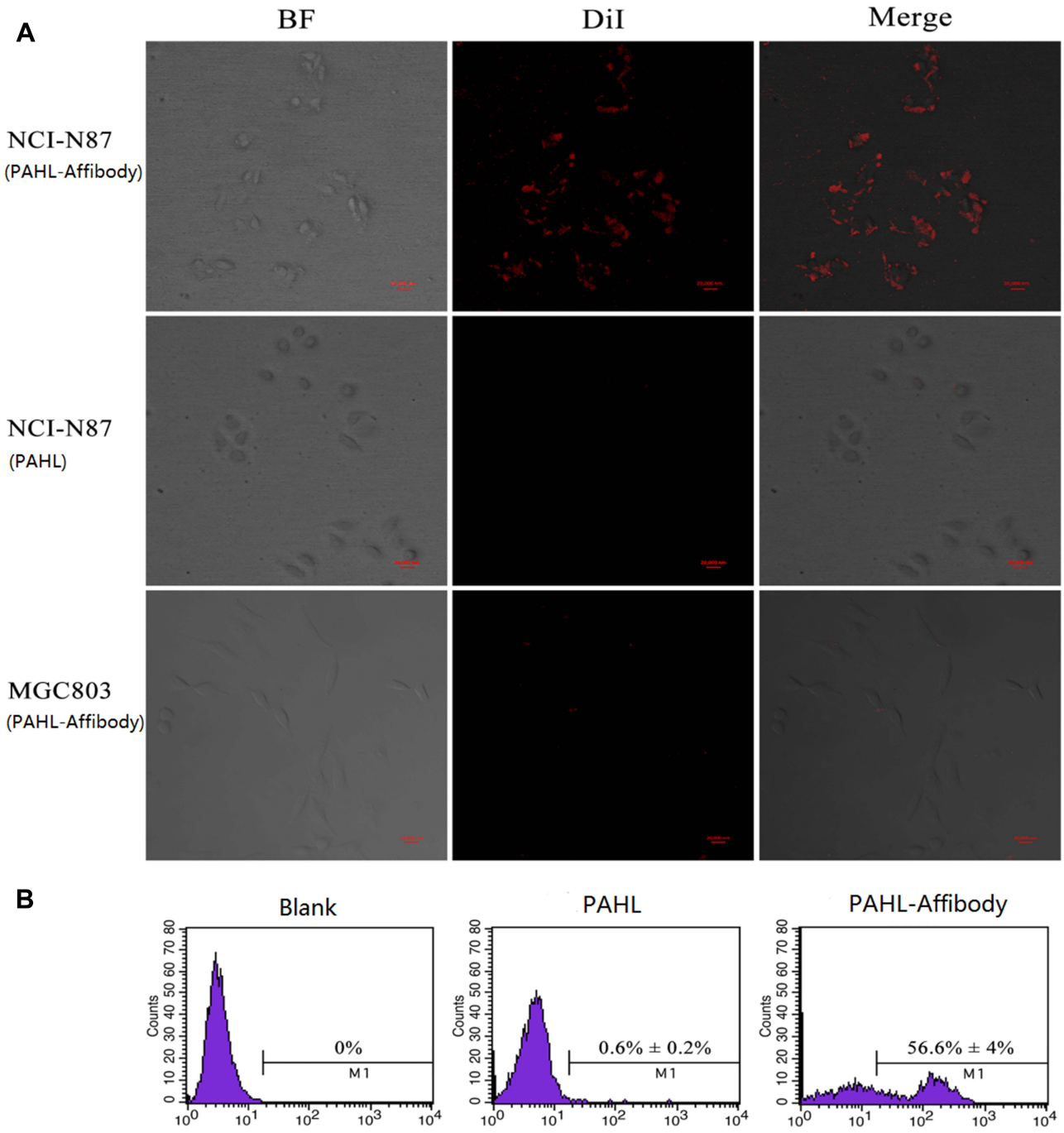

Figure 3 In vitro targeting ability of PAHL conjugates. (**A**) LSCM images of NCI-N87 cells incubated with PAHL-Affibody (top), NCI-N87 cells incubated with PAHL (without Affibody; middle), and MGC803 cells incubated with PAHL-Affibody (bottom). (**B**) FCM analysis of NCI-N87 cells (blank control, left), NCI-N87 cells incubated with PAHL (without Affibody, middle), and NCI-N87 cells incubated with PAHL-Affibody (right). Scale bar represents 20 μm.

cm2, and the frequency was 650 KMZ. It was found that the survival rate of gastric cancer cells was above 90% when the irradiation time was less than 60 s (Figure 6A). Longer period caused significant death of cells. Therefore, an optimized irradiation time of 60 s was chosen in our study.

Nuclear Localization Effect of PAHL-Affibody Nano UCA

In this study, laser scanning confocal microscopy was used to observe the distribution of Cy5-labeled HSV-TK in cells, and whether the suicide gene (HSV-TK) could be successfully delivered into the nucleus by low-frequency ultrasound

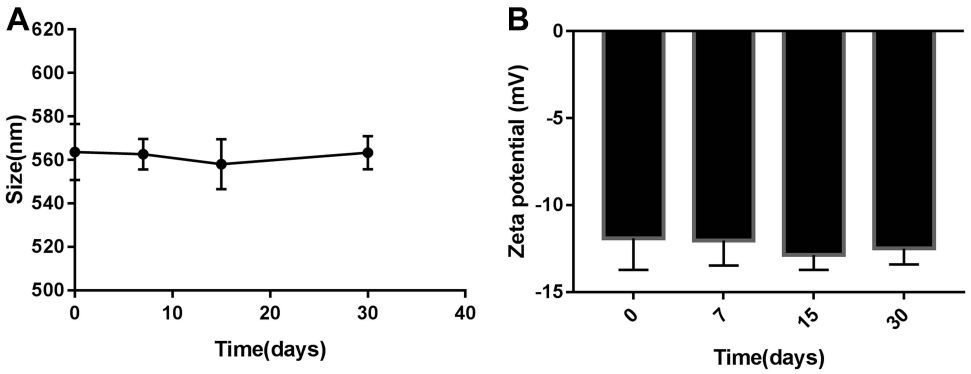

Figure 4 Particle size (**A**) and zeta potential (**B**) of PAHL after storage for different periods of time. Values were measured at day 0, day 7, day 15, day 30. Data represent mean ± SD (n=3).

instrument (ie UTMD technology) combined with PAHL-Affibody nano UCA. As shown in Figure 7, red fluorescence represents Cy5 labeled HSV-TK, and blue fluorescence represents Hochest33342 labeled nucleus. After transfection for 4 hours, red fluorescence could be observed in almost all cells, indicating that HSV-TK was successfully delivered into the cells.

Inhibitory Effect of PAHL-Affibody Nano UCA Combined with Low Frequency Ultrasound on Proliferation of ErbB2 (+) Gastric Cancer Cells

First, we determined the optimal concentration of GCV used in the PAHL formulations for transfection study. The concentrations of GCV were set as 5000, 2000, 1000, 500, 200, 100, 50, and 20 μg/mL in the MTT assay. The results showed that when the GCV concentration was higher than 500 μg/mL, significant cytotoxic effect was found in cancer cells (Figure 6B). When the GCV concentration was less than 200 μg/mL the cell survival rate was more than 90% (Figure 6B), which could be regarded as having no significant effect on cells. In this study, the optimal concentration of GCV was selected as 200 μg/mL in order to maintain the maximum biological effect and the minimum cytotoxic effect of GCV.

The effect of the prepared PAHL formulations on the survival of ErbB2 positive gastric cancer cells was studied by MTT assay (Figure 6C). It was found that the cell survival rates of Treatment A group Treatment B group were 92.13% and 90.56%, respectively. There was no significant statistical difference between these two treatment groups ($p > 0.05$), suggesting that the raw materials of nano UCAs in this study were relatively safe for the cells. The cell survival rate of Treatment C group was significantly reduced to 70.30%, compared to the former two treatment groups ($p < 0.05$). The cell survival rate of the Treatment D group was further reduced to 36.24%, which was significantly different compared to the treatment without ultrasound irradiation ($p < 0.05$) (Figure 6C).

As shown in the results from flow cytometry (Figure 8), the apoptosis rates of blank nano UCAs and ErbB2 targeted blank nano UCAs group connected with Affibody (without ultrasound irradiation) were only 10.9% and 12.13%, respectively. The apoptosis rate of PAHL-Affibody nano UCA (without ultrasound irradiation) was significantly increased to 45%. After combining with UTMD technology, PAHL-Affibody nano UCA (with ultrasound irradiation) continued to increase the apoptosis effect on tumor cells with the best apoptosis rate of 67% (Figure 8). These cell apoptosis results from flow cytometry were consistent with the prior MTT results.

Discussion

The purpose of this study was to prepare and evaluate a novel PAHL-Affibody nano UCA that can be used as a treatment of ErbB2 positive gastric cancer. First, the polyplexes of AGM-CBA/HSV-TK were prepared, the surface zeta potential of which was positive due to the cationic non-viral gene delivery vector (AGM-CBA). Next, in order to prepare uniform nano-scale liposomes, surfactants were required in solution or high-speed centrifugation should be applied to liposome suspensions,[27,28] resulting in a reduction of the stability and yield of nano-scaled liposomes. In

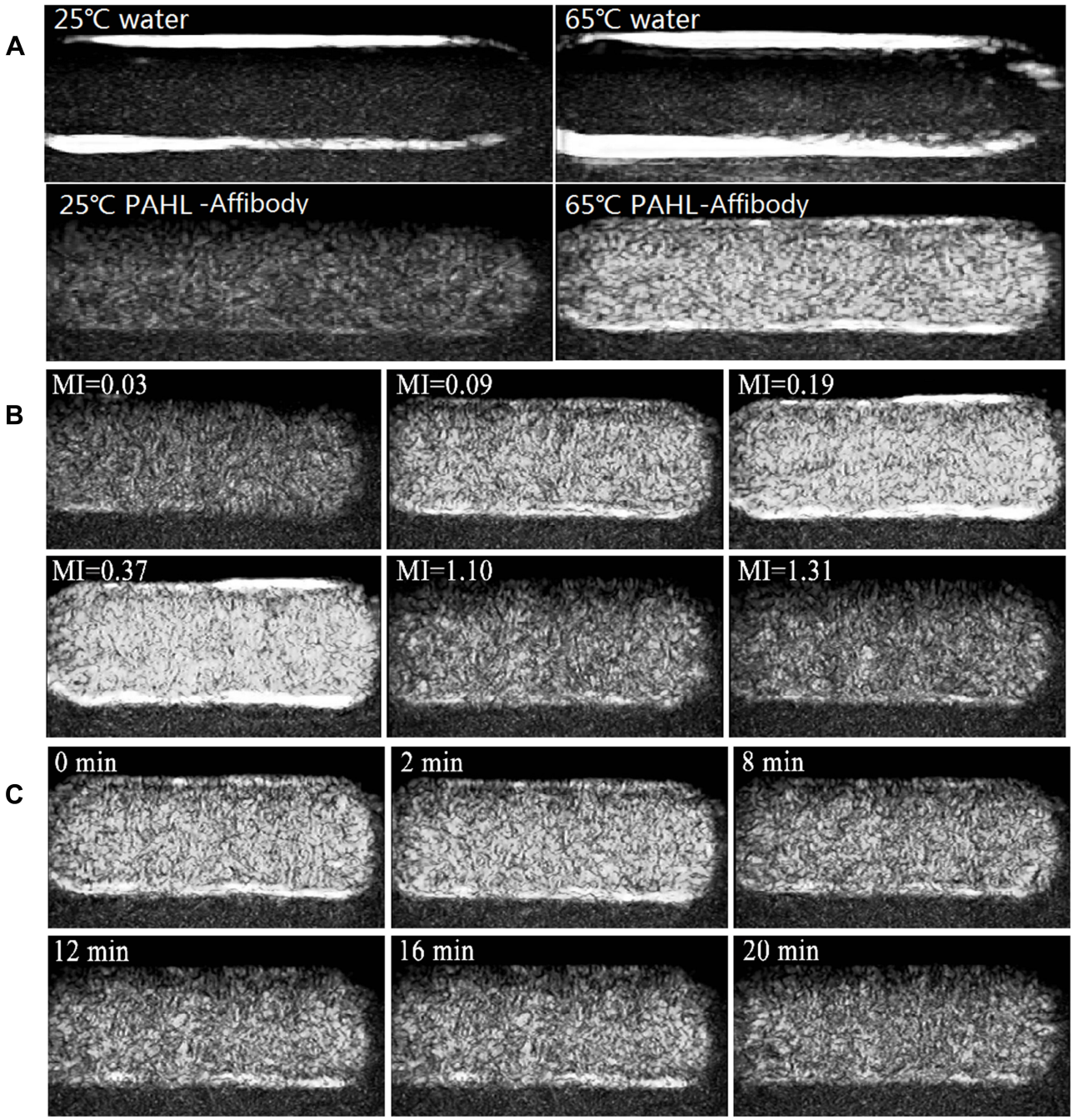

Figure 5 In vitro ultrasound images of (**A**) PAHL (7.3 mg/mL) and degassed water at two different temperatures (25 and 65°C) using CEUS mode. (**B**) PAHL diluted in degassed water (7.3 mg /mL) at different MI values using CEUS mode. (**C**) PAHL (7.3 mg/mL) at different time intervals using CEUS mode (MI of 0.09).

this study, a nano UCA was obtained based on a simple method described in the section of materials and methods. Our results showed that the average particle size of the PAHL–Affibody was 560 ± 4.8nm with PDI = 0.197 ± 0.038. In contrast, the mean diameter of the SonoVue MBs was 2176.3 ± 403.3 nm with PDI = 0.190 ± 0.032.[20] The PDI of the PAHL–Affibody and SonoVue MBs were nearly consistent. According to the instruction manual of the zeta potential/nanometer particle size analyzer, a low PDI value indicates high homogeneity in the size of the particle. As such, the negatively charged DSPE-PEG (2000) was used as one of the constituents of the shell of the nano UCAs, so the PAHL–Affibody was negatively charged as a whole like the SonoVue MBs to ensure its stability in water.[20,29] At the

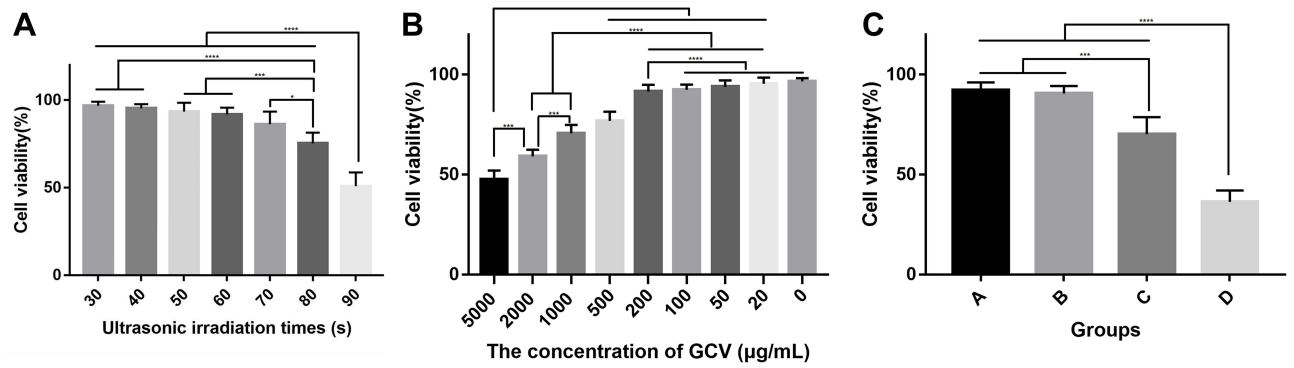

Figure 6 (**A**) Survival rate of cells treated by low-frequency ultrasound with different irradiation times. Data represent mean ± SD (n=5). (**B**) Survival rate of cells treated by GCV with different concentrations. Data represent mean ± SD (n=5). (**C**) Survival rate of NCI-N87 cells treated by A: Treatment A - blank nano UCA (without AGM-CBA /HSV-TK and ultrasound irradiation), B: Treatment B - Affibody-connected ErbB2 targeted blank nano UCA (without AGM-CBA/HSV-TK and ultrasound irradiation), C: Treatment C - PAHL-Affibody nano UCA (without ultrasound irradiation), D: Treatment D - PAHL-Affibody nano UCA (with ultrasound irradiation). Data represent mean ± SD (n=5). *P < 0.05 compared with each other. ***P < 0.001 compared with each other.****P < 0.0001 compared with each other.

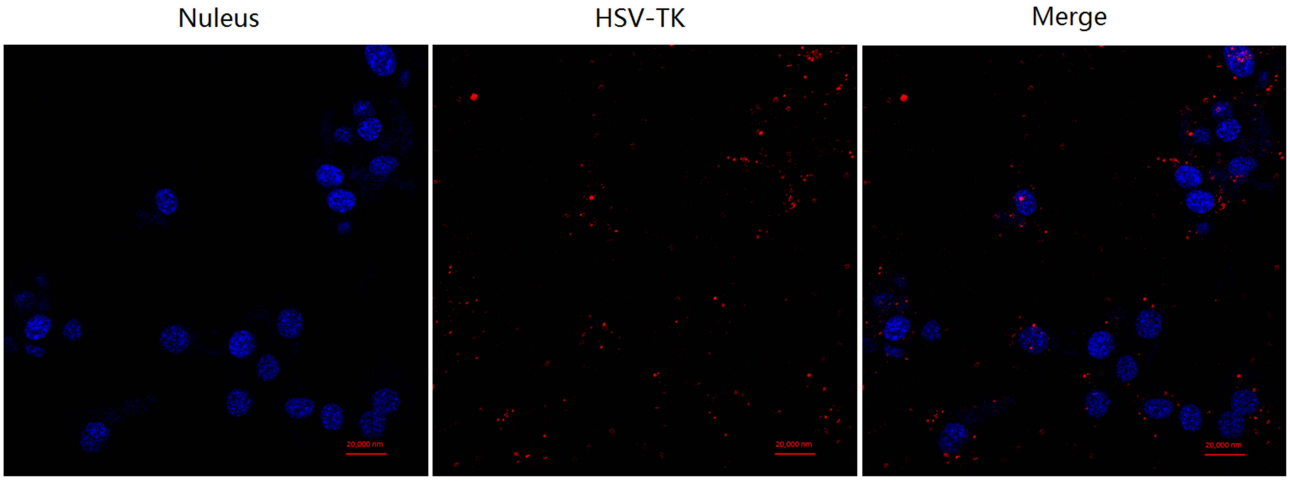

Figure 7 Nuclear localization effect of PAHL-Affibody nano UCA in NCI-N87 cells. The cells transfected with PAHL consisted of Cy5-pHSV-TK (in red color) for 4 h at 37°C. The cell nuclei were stained with Hoechst 33,342 (in blue color). Scale bar represents 20 μm. Scale bar represents 20 μm.

same time, DSPE-PEG (2000) can assist in producing a nano UCA with good dispersibility and biocompatibility in water.[30]

Finally, a currently widely used biotin-avidin method was used to conjugate Affibody that specifically targets the ErbB2 molecules with PAHL nano UCAs. We used biotinylated DSPE-PEG-2000 as one of the components of the shell of nano UCAs, Affibody as a ligand of the biotinylated anti-tumor ErbB2 molecule, and streptavidin as a bridge substance coupling the former two entities. Streptavidin is a protein similar to avidin. In structure, it exists as a homotetramer. Each mole of the tetramer molecule can bind to four moles of biotin molecules. The affinity of the coupling is far greater than that of avidin. Therefore, we selected streptavidin to successfully connect the biotinylated nano UCAs with biotinylated anti-ErbB2 Affibody molecules. Biotinylated DSPE-PEG-2000 is a type of micelle-like hydrophilic polymer phospholipids,[31,32] and the dispersibility and re-modification of nano UCAs can be greatly increased by adding DSPE-PEG into the shell of the nano UCAs.[29]

Functionally, the affibody mimics the monoclonal antibody. Compared with antibody, the biggest difference between the anti-ErbB2 Affibody and ErbB2 antibody is that the Affibody has a smaller size. The molecular weight of the anti-ErbB2 Affibody molecules is 6 kDa, while the molecular weight of ErbB2 antibody is 150 kDa. Affibody can make the volume of PAHL small enough to enter the tumor tissue directly through the gap between tumor neovascular

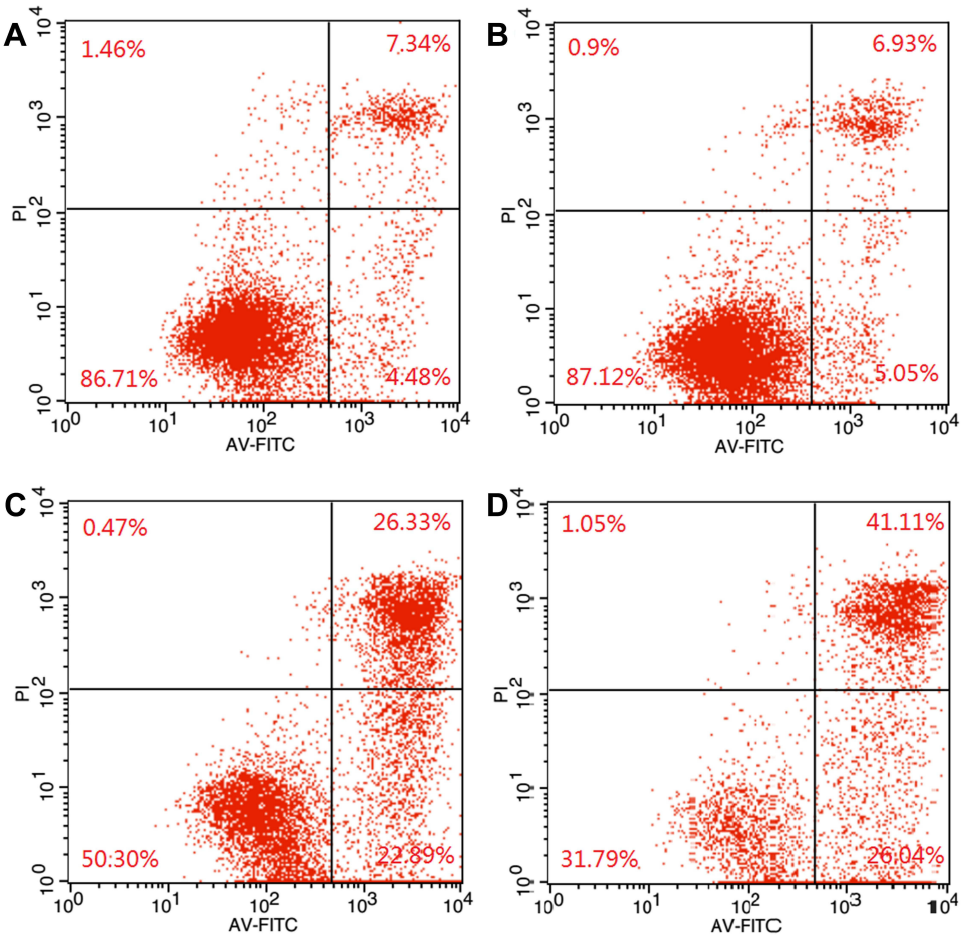

Figure 8 Apoptosis rate of NCI-N87 gastric cancer cells treated by (**A**) blank nano UCAs group, (**B**) affibody-connected ErbB2 targeted blank UCAs group (without ultrasound irradiation), (**C**) PAHL-Affibody nano UCA (without ultrasound irradiation), (**D**) PAHL-Affibody nano UCA (with ultrasound irradiation).

endothelial cells, and the unique physical properties of Affibody make it able to withstand various conditions including extreme pH and high temperature. Despite its smaller size, the binding site of the Affibody is similar to that of the antibody, and the affinity of the Affibody to the ligand is significantly higher than that of the antibody.[33] It has been shown that Affibody molecules can also achieve effective penetration and rapid biological distribution in rats and mice, so that affibody molecules can quickly find and connect to targets within 1 hour.[34] All of these unique characteristics of the Affibody molecules make PAHL–Affibody conjugate more advantageous in both in vitro and in vivo research works.

Affibody is a new type of synthetic affinity ligand that is similar to antibody in function. However, there is no corresponding fluorescent secondary antibody for Affibody, and there is no easy approach to directly detect the connection between Affibody and nano UCAs. Therefore, by detecting the connection between the PAHL-Affibody with red fluorescent dye imbedded in the liposomal components and ErbB2 (+) gastric cancer cells, we indirectly verified that Affibody was successfully linked with PAHL nano UCAs, and it could target the ErbB2 (+) gastric cancer cells. In addition, the particle size of PAHL-Affibody is larger than that of PAHL and the zeta potential of PAHL-Affibody is lower than that of PAHL, which can also prove the successful connection of Affibody and PAHL nano UCAs to a certain extent.

In order to utilize the contrast diagnostic function of the prepared PAHL-Affibody nano UCA in gastric cancerous lesions in vivo, it is necessary to investigate the ultrasound-induced phase change conditions and stability (ie, the duration of contrast image) of the PAHL-Affibody nano UCA.[35] In this study, we investigated the effects of two relevant parameters (temperature and mechanical index) on the ultrasound imaging of PAHL-Affibody nano UCA. It was found

that the ultrasound contrast effect of PAHL –Affibody nano UCA at 65°C was significantly better than that at room temperature (25°C). It has been reported that gastric cancer cells have higher temperature than normal cells due to obvious enhancement of metabolic activity.[36] This is actually more conducive to promoting the phase change of the prepared PAHL-Affibody nano UCA, thus producing better ultrasound contrast effect. Overall, with 65°C temperature and a mechanical index of 0.09, the prepared PAHL-Affibody nano UCA demonstrated applicable ultrasound diagnostic capability.

Nuclear membrane was another obstacle for gene delivery. Only when potential therapeutic genes successfully enter the nucleus can the following transcription and translation be carried out, thus successfully realizing gene delivery. In this study, laser scanning confocal microscopy was used to observe the distribution of Cy5-labeled HSV-TK in cells. It was worth noting that some of the red fluorescence and blue fluorescence in the transfected cells coincided with each other and were shown pink on the photographs of laser scanning confocal microscope, which further indicated that HSV-TK had been successfully delivered into the cells. This was due to the intracellular localization effect of guanidine polymers AGM-CBA, whose nuclear localization ability had been reported previously.[9,11,37,38] This greatly assisted the delivery of HSV-TK into the nucleus and led to further successful transfection.

Our study indicated that PAHL-Affibody nano UCA combined with low-frequency ultrasound irradiation, ie UTMD technology, had significantly enhanced anti-cell proliferation ability, which was greatly superior to the PAHL-Affibody nano UCA without ultrasound irradiation. On the one hand, the cavitation effect generated by UTMD caused a series of physical processes, such as oscillation, swelling, compression and implosion of PAHL, resulting in the rapid release of the polyplexes of AGM-CBA/HSV-TK at the site of ultrasound irradiation and the local aggregation of the polyplexes of AGM-CBA/HSV-TK in the tumor cells. On the other hand, microbubbles containing the polyplexes of AGM-CBA/HSV-TK were used as cavitation nucleus. The cavitation was stable and continued to generate "acoustic pore effect" under the action of ultrasound, which caused the cell membrane of adjacent cells to form pores. This could increase the permeability of the cell membrane and facilitate the polyplexes of AGM-CBA/HSV-TK to enter tumor cells. This effect not only led to increased transfection efficiency of target genes in the cells but also improved targeting and accuracy of gene therapy, and enhanced anti-tumor effect without damages to the transfected genes.

Apoptosis plays a negative regulatory role in the occurrence and development of tumors. In our study, PAHL-Affibody nano UCA (with ultrasound irradiation) demonstrated the best effect on inducing tumor death/apoptosis, which further confirmed that the polyplexes of AGM-CBA/HSV-TK release could induce cell apoptosis in targeted nano UCAs after ultrasound blasting.

However, this study still has several limitations. First, this study failed to deeply investigate the mechanism by which UTMD technology promotes gene transfection and to explore whether it affects the "bystander tumor cell killing" mechanism of the HSV-TK/GCV system. Second, This study did not study the antitumor and safety of the PAHL-Affibody nano UCA in animals. Our research group will further study.

Conclusions

In the field of ultrasound molecular imaging and targeted therapy of tumors, nano UCA is a newly emerging approach with many advantages and great research and clinical significance. At present, there has not been any research on the construction of gene-carrying UCAs for the targeted therapy of gastric cancer.

Compared with other studies, we developed ErbB2 targeted nano UCAs containing both the polyplexes of AGM-CBA/HSV-TK and PFH, which could be triggered to have phase change by ultrasound, therefore increasing the targeted gene delivery. In this system, we used our laboratory's research results, guanidinylated SS-PAAs polymer (AGM-CBA), as the nuclear localization vector of the suicide genes, and then used ErbB2 targeted nano UCAs as the targeted vector of genes. Uniform and nanoscaled UCA was successfully conjugated with biotinylated Affibody molecule, which not only had small size but also demonstrated high affinity and specificity for ErbB2 molecules overexpressed in gastric cancer cells. With the aid of ultrasound, the nano UCAs went through phase change and became microbubbles, resulting in a better in vitro ultrasound contrast effect. In addition, the ultrasound targeted microbubble destruction technology and the nuclear localization effect of AGM-CBA jointly improved the transfection efficiency of suicide genes in gastric

cancer cells, and significantly caused apoptosis of gastric cancer cells. More studies are still needed to further test the in vivo application of PAHL-Affibody nano UCA in ultrasound imaging and targeted therapy for gastric cancer.

Acknowledgments

The work received financial supports from the National Natural Science Foundation of China (Grant Number 81801712, 81872822) and Liaoning Provincial Education Department 2019 Annual Scientific Research Funding Project Foundation (Grant number 2019LJC07).

Disclosure

The authors declare no conflicts of interest.

References

1. Sano T. Gastric cancer: Asia and the world. *Gastric Cancer*. 2017;20(Suppl 1):1–2. doi:10.1007/s10120-017-0694-9
2. Strong VE. Progress in gastric cancer. *Updates Surg*. 2018;70(2):157–159. doi:10.1007/s13304-018-0543-3
3. Karjoo Z, Chen X, Hatefi A. Progress and problems with the use of suicide genes for targeted cancer therapy. *Adv Drug Deliv Rev*. 2016;99(Pt A):113–128. doi:10.1016/j.addr.2015.05.009
4. Aoi A, Watanabe Y, Mori S, Takahashi M, Vassaux G, Kodama T. Herpes simplex virus thymidine kinase-mediated suicide gene therapy using nano/microbubbles and ultrasound. *Ultrasound Med Biol*. 2008;34(3):425–434. doi:10.1016/j.ultrasmedbio.2007.09.004
5. Chen ZH, Yu YP, Zuo ZH, et al. Targeting genomic rearrangements in tumor cells through Cas9-mediated insertion of a suicide gene. *Nat Biotechnol*. 2017;35(6):543–550. doi:10.1038/nbt.3843
6. Greco R, Oliveira G, Stanghellini MT, et al. Improving the safety of cell therapy with the TK-suicide gene. *Front Pharmacol*. 2015;6:95. doi:10.3389/fphar.2015.00095
7. Walther W, Stein U. Viral vectors for gene transfer: a review of their use in the treatment of human diseases. *Drugs*. 2000;60(2):249–271. doi:10.2165/00003495-200060020-00002
8. Xue XY, Mao XG, Zhou Y, et al. Advances in the delivery of antisense oligonucleotides for combating bacterial infectious diseases. *Nanomedicine*. 2018;14(3):745–758. doi:10.1016/j.nano.2017.12.026
9. Liu H, Yang Z, Xun Z, et al. Nuclear delivery of plasmid DNA determines the efficiency of gene expression. *Cell Biol Int*. 2019;43(7):789–798. doi:10.1002/cbin.11155
10. Yang Z, Sun Y, Xian L, et al. Disulfide-bond-containing agmatine-cystaminebisacrylamide polymer demonstrates better transfection efficiency and lower cytotoxicity than polyethylenimine in NIH/3T3 cells. *J Cell Biochem*. 2018;119(2):1767–1779. doi:10.1002/jcb.26338
11. Yu J, Zhang J, Xing H, et al. Novel guanidinylated bioresponsive poly(amidoamine)s designed for short hairpin RNA delivery. *Int J Nanomedicine*. 2016;11:6651–6666.
12. Jiang N, Chen Q, Cao S, et al. Ultrasound targeted microbubbles combined with a peptide nucleic acid binding nuclear localization signal mediate transfection of exogenous genes by improving cytoplasmic and nuclear import. *Mol Med Rep*. 2017;16(6):8819–8825. doi:10.3892/mmr.2017.7681
13. Tay LM, Xu C. Coating microbubbles with nanoparticles for medical imaging and drug delivery. *Nanomedicine*. 2017;12(2):91–94. doi:10.2217/nnm-2016-0362
14. Methachan B, Thanapprapasr K. Polymer-based materials in cancer treatment: from therapeutic carrier and ultrasound contrast agent to theranostic applications. *Ultrasound Med Biol*. 2017;43(1):69–82. doi:10.1016/j.ultrasmedbio.2016.09.009
15. Tranquart F, Arditi M, Bettinger T, et al. Ultrasound contrast agents for ultrasound molecular imaging. *Z Gastroenterol*. 2014;52(11):1268–1276. doi:10.1055/s-0034-1384999
16. Vlaisavljevich E, Durmaz YY, Maxwell A, Elsayed M, Xu Z. Nanodroplet-mediated histotripsy for image-guided targeted ultrasound cell ablation. *Theranostics*. 2013;3(11):851–864. doi:10.7150/thno.6717
17. Lin L, Fan Y, Gao F, et al. UTMD-promoted co-delivery of gemcitabine and miR-21 inhibitor by dendrimer-entrapped gold nanoparticles for pancreatic cancer therapy. *Theranostics*. 2018;8(7):1923–1939. doi:10.7150/thno.22834
18. Chin LS, Lim M, Hung TT, Marquis CP, Amal R. Perfluorodecalin nanocapsule as an oxygen carrier and contrast agent for ultrasound imaging. *RSC Adv*. 2014;4(25):13052–13060. doi:10.1039/c3ra47595f
19. Zong L, Abe M, Seto Y, Ji J. The challenge of screening for early gastric cancer in China. *Lancet*. 2016;388(10060):2606. doi:10.1016/S0140-6736(16)32226-7
20. Gao D, Gao J, Xu M, et al. Targeted ultrasound-triggered phase transition nanodroplets for Her2-overexpressing breast cancer diagnosis and gene transfection. *Mol Pharm*. 2017;14(4):984–998. doi:10.1021/acs.molpharmaceut.6b00761
21. Yang H, Cai W, Xu L, et al. Nanobubble-Affibody: novel ultrasound contrast agents for targeted molecular ultrasound imaging of tumor. *Biomaterials*. 2015;37:279–288. doi:10.1016/j.biomaterials.2014.10.013
22. Zhang Y, Wan CF, Du J, et al. The in vitro study of Her-2 targeted gold nanoshell liquid fluorocarbon poly lactic-co-glycolic acid ultrasound microcapsule for ultrasound imaging and breast tumor photothermal therapy. *J Biomater Sci Polym Ed*. 2018;29(1):57–73. doi:10.1080/09205063.2017.1399003
23. Zhu L, Guo Y, Wang L, et al. Construction of ultrasonic nanobubbles carrying CAIX polypeptides to target carcinoma cells derived from various organs. *J Nanobiotechnology*. 2017;15(1):63. doi:10.1186/s12951-017-0307-0
24. Zhang H. Thin-film hydration followed by extrusion method for liposome preparation. *Methods Mol Biol*. 2017;1522:17–22.
25. Wang M, Hu H, Sun Y, et al. A pH-sensitive gene delivery system based on folic acid-PEG-chitosan - PAMAM-plasmid DNA complexes for cancer cell targeting. *Biomaterials*. 2013;34(38):10120–10132. doi:10.1016/j.biomaterials.2013.09.006

26. Liu H, Sun Y, Lang L, et al. Nuclear localization signal peptide enhances transfection efficiency and decreases cytotoxicity of poly(agmatine/N,N'-cystamine-bis-acrylamide)/pDNA complexes. *J Cell Biochem*. 2019;120(10):16967–16977. doi:10.1002/jcb.28958
27. Krupka TM, Solorio L, Wilson RE, et al. Formulation and characterization of echogenic lipid-Pluronic nanobubbles. *Mol Pharm*. 2010;7(1):49–59. doi:10.1021/mp9001816
28. Xing Z, Wang J, Ke H, et al. The fabrication of novel nanobubble ultrasound contrast agent for potential tumor imaging. *Nanotechnology*. 2010;21(14):145607. doi:10.1088/0957-4484/21/14/145607
29. Carion O, Mahler B, Pons T, Dubertret B. Synthesis, encapsulation, purification and coupling of single quantum dots in phospholipid micelles for their use in cellular and in vivo imaging. *Nat Protoc*. 2007;2(10):2383–2390. doi:10.1038/nprot.2007.351
30. Gao J, Chen K, Miao Z, et al. Affibody-based nanoprobes for HER2-expressing cell and tumor imaging. *Biomaterials*. 2011;32(8):2141–2148. doi:10.1016/j.biomaterials.2010.11.053
31. Ito A, Ino K, Kobayashi T, Honda H. The effect of RGD peptide-conjugated magnetite cationic liposomes on cell growth and cell sheet harvesting. *Biomaterials*. 2005;26(31):6185–6193. doi:10.1016/j.biomaterials.2005.03.039
32. Verma A, Stellacci F. Effect of surface properties on nanoparticle-cell interactions. *Small*. 2010;6(1):12–21. doi:10.1002/smll.200901158
33. Nygren PA. Alternative binding proteins: affibody binding proteins developed from a small three-helix bundle scaffold. *FEBS J*. 2008;275(11):2668–2676. doi:10.1111/j.1742-4658.2008.06438.x
34. Tolmachev V, Rosik D, Wallberg H, et al. Imaging of EGFR expression in murine xenografts using site-specifically labelled anti-EGFR 111In-DOTA-Z EGFR:2377 Affibody molecule: aspect of the injected tracer amount. *Eur J Nucl Med Mol Imaging*. 2010;37(3):613–622. doi:10.1007/s00259-009-1283-x
35. Rapoport N, Christensen DA, Kennedy AM, Nam KH. Cavitation properties of block copolymer stabilized phase-shift nanoemulsions used as drug carriers. *Ultrasound Med Biol*. 2010;36(3):419–429. doi:10.1016/j.ultrasmedbio.2009.11.009
36. Hiruta Y, Funatsu T, Matsuura M, Jian W, Kanazawa H. PH/temperature-responsive fluorescence polymer probe with pH-controlled cellular uptake. *Sens Actuators B Chem*. 2015;207:724–731. doi:10.1016/j.snb.2014.10.065
37. Yu J, Zhang J, Xing H, et al. Guanidinylated bioresponsive poly(amido amine)s designed for intranuclear gene delivery. *Int J Nanomed*. 2016;11:4011–4024. doi:10.2147/IJN.S115773
38. Kim TI, Lee M, Kim SW. A guanidinylated bioreducible polymer with high nuclear localization ability for gene delivery systems. *Biomaterials*. 2010;31(7):1798–1804. doi:10.1016/j.biomaterials.2009.10.034